pH Response of Model Diblock and Triblock Copolymer Networks Containing Polystyrene and Poly(2-hydroxyethyl methacrylate-*co*-2-(dimethylamino)ethyl methacrylate)

Kyle B. Guice,[†] Stephen R. Marrou,[†] Sudershan R. Gondi,[‡] Brent S. Sumerlin,[‡] and Yueh-Lin Loo*[,§]

Department of Chemical Engineering, University of Texas at Austin, Austin, Texas 78712; Department of Chemistry, Southern Methodist University, Dallas, Texas 75275; and Department of Chemical Engineering, Princeton University, Princeton, New Jersey 08544

Received February 19, 2008; Revised Manuscript Received April 13, 2008

ABSTRACT: We investigated the swelling behavior of lamella-forming diblock and triblock copolymers of polystyrene, PS, and poly(2-hydroxyethyl methacrylate-*co*-2-(dimethylamino)ethyl methacrylate), PHD, with varying 2-(dimethylamino)ethyl methacrylate (DMAEMA) content. In phosphate buffer solutions of varying pH's, these model networks swell like cationic hydrogels; their swelling characteristics are tunable through the DMAEMA content within the PHD block. While glassy PS domains within PS/PHD/PS can serve as physical cross-links in triblock copolymer networks, the PS domains are not effective anchors in diblock copolymer networks. PS/PHD with high DMAEMA content thus macroscopically disintegrate upon protonation of DMAEMA. The lamellar microdomains within these networks, however, continue to swell with decreasing pH. By reducing the DMAEMA content in PS/PHD, we have been able to create a diblock copolymer network that is macroscopically stable upon protonation of DMAEMA, as its water uptake cannot induce sufficient osmotic pressure to break up the sample. The swelling characteristics of this particular network mirror those of physically cross-linked PS/PHD/PS networks with comparable DMAEMA content.

Introduction

Stimuli-responsive hydrogels are being investigated for a range of applications, including adaptive lenses,[1] nanofiltration,[2,3] gene[4] and drug delivery,[5–8] and tissue scaffolds.[9] Polymers containing 2-(dimethylamino)ethyl methacrylate, DMAEMA, are responsive to both pH[4] and temperature.[8] As such, DMAEMA-containing hydrogels are being widely explored for these applications.[1–9] To further tailor the response properties of hydrogels, DMAEMA is often copolymerized with other monomers.[5,9–12] In particular, 2-hydroxyethyl methacrylate, HEMA, a monomer that is biocompatible and is moderately water-swellable in its polymeric form, has been widely studied as a comonomer to tune the properties of DMAEMA-based hydrogels.[1,5,6,8,9,11–14] For example, a 10% increase in the HEMA content in poly(HEMA-*co*-DMAEMA) hydrogels can decrease the rate of diffusion of protamine through these gels by a factor of 3.[5]

While the hydrogel materials that have been previously described are undoubtedly useful, fundamental study of these systems is limited by characteristically large composition distributions within the gels.[15] Specifically, synthetic limitations have resulted in nonuniform compositional distributions even for two-component hydrogels (e.g., monomer and cross-linker).[15–18] The incorporation of additional monomer types further complicates the composition distribution within the gels.[19] In some cases, wide composition distributions within hydrogels can result in phase separation.[15] Even in cross-linked hydrogels that do not exhibit phase separation, nonuniformities in the cross-link distribution can significantly impact their swelling properties. For example, increasing the nonuniformity in the cross-link distribution of cured epoxy resins resulted in a 2-fold increase in their solvent uptake.[20]

Recently, research has sought to minimize heterogeneities in the cross-link distributions of hydrogels through the use of model network architectures.[21–30] Typically, these model networks are derived from amphiphilic block copolymers, with the glassy hydrophobic blocks serving as physical cross-links.[21,29] Utilizing microphase separation,[31] amphiphilic block copolymers can self-assemble to form a variety of well-ordered microstructures (e.g., lamallae, gyroids, cylinders, or spheres) in the bulk.[28–33] Given that the swelling behavior of microphase-separated amphiphilic triblock copolymer networks can depend strongly on the details of the microstructure, the use of block copolymers provides another parameter with which one can tune their properties.[28]

Controlled-free radical polymerization techniques, which allow one to design polymers with narrow molecular weight distributions and controlled molecular weights, are critical to the design of model networks.[21,29] A variety of these controlled free-radical polymerization techniques, including atom transfer radical polymerization, ATRP,[35,36] and reversible addition−fragmentation chain transfer polymerization, RAFT,[37–44] have been shown to yield poly(DMAEMA) homopolymers and DMAEMA-containing block copolymers of controlled molecular weights and narrow molecular weight distributions.[45–53] Previously, we have also demonstrated that poly(HEMA-*co*-DMAEMA) statistical copolymers can be synthesized with controlled comonomer distributions by the selection of an appropriate solvent for polymerization.[45,46] Further, we have also shown that block copolymers containing compositionally uniform poly(HEMA-*co*-DMAEMA) can be synthesized with controlled molecular weights and narrow molecular weight distributions.[45,54] These materials have been demonstrated to microphase separate to form well-ordered microstructures in the solid state.[45,54]

In this work, we investigated the pH response of model networks derived from lamella-formers of polystyrene-*b*-poly(HEMA-*co*-DMAEMA), PS/PHD. The hydrophobic PS microdomains are glassy during the course of the swelling experiments. Of specific relevance to this study is whether or not the

* Corresponding author. E-mail: lloo@princeton.edu.
[†] University of Texas at Austin.
[‡] Southern Methodist University.
[§] Princeton University.

10.1021/ma8003746 CCC: $40.75 © 2008 American Chemical Society
Published on Web 05/22/2008

glassy PS microdomains can effectively serve as physical cross-links to lock in the solid-state morphology in model networks. It has been widely assumed that only amphiphilic block copolymers containing two or more glassy, hydrophobic blocks (i.e., at least a triblock copolymer architecture) can retain their morphologies during swelling. The glassy microdomains are crucial as they serve to anchor the swellable component on both ends.[21–28] The swelling behavior of model networks in which the swellable component is not anchored at both ends, however, has not been looked into carefully. In this paper, we compare the swelling characteristics of PS/PHD/PS triblock and PS/PHD diblock copolymer networks at varying PHD compositions in order to probe the limits of the swelling of diblock copolymer networks. Further, we demonstrate the tunability of the swelling characteristics of these block copolymer networks by controlling the DMAEMA content.

Experimental Section

Materials. HEMA (Acros, 98%) was vacuum-distilled (40 mTorr, 65 °C) to remove ethylene glycol dimethacrylate[55] and stored at 0 °C prior to use. DMAEMA (Acros, 98%) and styrene (Acros, 98%) were passed through columns of activated basic alumina and stored at 0 °C prior to use. Ethyl α-bromoisobutyrate (EB*i*B, Aldrich, 98%), *N*,*N*,*N*′,*N*″,*N*″-pentamethyldiethylenetriamene (PMDETA, Aldrich, 99%), Cu(I)Br (Aldrich, 98%), Cu(II)Br (Acros, anhydrous 99%), Cu(I)Cl (Acros, 99%), Cu(II)Cl_2 (Acros, 99%), 2,2′-azobis(isobutyronitrile) (AIBN, Aldrich, 98%), *N*,*N*-dimethylformamide (DMF, Acros), and dimethyl sulfoxide (DMSO, extra dry, Fisher Scientific) were used as received.

Synthesis of Cumyl Dithiobenzoate. Cumyl dithiobenzoate (CDB), the monofunctional RAFT chain transfer agent used in our study, was prepared following a method similar to that of Oae et al.[56] Specifically, dithiobenzoic acid[57] (11.1 g, 72.0 mmol) and α-methylstyrene (10.4 g, 88.0 mmol) were dissolved in carbon tetrachloride (40 mL), and the resulting solution was purged with nitrogen and stirred at 70 °C for 5 h. The crude product was obtained as a dark purple oil in 69% yield and was subsequently purified by column chromatography with neutral alumina as the packing material and hexanes as the eluent.

Synthesis of 1,3-Bis(2-(thiobenzoylthio)prop-2-yl)benzene (TBTPB).[58] TBTPB is the bifunctional RAFT chain transfer agent used in our study. To prepare TBTPB, dithiobenzoic acid (20.0 g, 130 mmol), 1,3-diisopropenylbenzene (10.3 g, 64.8 mmol), and a catalytic amount of *p*-toluenesulfonic acid (1.0 g) were dissolved in carbon tetrachloride (80 mL). The resulting solution was heated at 70 °C for 18 h under a nitrogen atmosphere. The reaction mixture was cooled to room temperature, and a saturated solution of sodium bicarbonate (100 mL) was added. After extraction with dichloromethane (100 mL × 2), the organic layers were combined, washed with a saturated brine solution (200 mL), dried over $MgSO_4$ (10 g), and concentrated under reduced pressure to yield a red residual oil. Column chromatography with silica gel as the packing material and hexanes as the eluent yielded the product in 55% yield. ^{1}H NMR (400 MHz, $CDCl_3$): 7.75−7.69 (dd, 4H, J = 7.5 Hz, SPh-C2*H* and SPh-C6*H*), 7.36−7.32 (m, 3H, Ar−C5*H* and SPh-C4*H*), 7.30−7.28 (m, 2H, Ar−C4*H* and Ar−C6*H*), 7.24−7.16 (m, 5H, SPh-C3*H* and SPh-C5*H,* Ar−C2*H*), 1.89 (s, 12H, (Ar-*C*1-C[CH_3]$_2$). ^{13}C NMR (100.6 MHz, $CDCl_3$): 146.3 (Ph-*C*1-C═S), 143.7 (Ar-*C*1-C[CH_3]$_2$), 131.5 (Ar-*C*5H), 128.1 Ar-*C*4H and Ar-*C*6H), 128.0 (SPh-*C*4H), 126.5 (SPh-*C*3H and SPh-*C*5H), 125.4 (Ar-*C*2H), 124.8 (SPh-*C*2H and SPh-*C*6H), 56.4 (Ar−C1-*C*[CH_3]$_2$), 28.3 (Ar−C1−C[*C*H_3]$_2$). IR (KBr; expressed in units of wavenumber, cm^{-1}): 3050, 2970 (C−Cs), 1589, 1444 (C═C), 1264, 1040 (C═S) 908, 765 cm^{-1} (C-Cb). Elemental analysis: Calculated for $C_{26}H_{26}S_4$: C, 66.91%; H, 5.61%. Found: C, 67.09%; H, 5.67%.

Polymerization Methods. For clarity, all PS/PHD diblock copolymers will be referred to as PS/PHD$_F$, where F is the composition (in mol %) of DMAEMA in the PHD block. Similarly, all triblock copolymers will be referred to as PS/PHD$_F$/PS. The synthesis of a PS macroinitiator and its subsequent initiation and polymerization to PS/PHD$_{28}$ by ATRP in DMF were previously described.[45] Copolymerization of HEMA and DMAEMA in DMF at the azeotropic composition (28 mol % DMAEMA) yielded statistical copolymers of PHD$_{28}$. To make block copolymers containing PHD of compositions other than that of the azeotropic composition, we carried out HD copolymerizations in DMSO, where the reactivity ratios of HEMA and DMAEMA are near unity.[46] We were, however, unable to synthesize PS/PHD block copolymers from PS macroinitiators in DMSO because PS does not readily dissolve in DMSO. While one can in principle first polymerize PHD macroinitiators in DMSO and then use these macroinitiators to initiate the polymerization of the second block in a good solvent for PS, halogen end-group loss with DMAEMA and/or HEMA during macroinitiator cleanup prevents the subsequent initiation of a second block by PHD.[59] We therefore developed an alternate synthetic route to synthesize PS/PHD diblock and triblock copolymers using RAFT. RAFT has been demonstrated as a robust technique for the synthesis of DMAEMA-containing polymers.[21] Accordingly, only PS/PHD$_{28}$ diblock copolymer was synthesized by ATRP from a PS macroinitiator per earlier reports,[45] and all the other diblock and triblock copolymers used in this study were synthesized by RAFT.

The RAFT copolymerizations of DMAEMA and HEMA were carried out with either monofunctional (CDB; for the synthesis of diblock copolymers) or bifunctional (TBTPB; for the synthesis of triblock copolymers) chain transfer agents (CTA) at a total monomer:CTA:AIBN molar ratio of 250:5:1. Each copolymerization utilized 20 g of total monomer (HEMA and DMAEMA) diluted in 40 mL of DMSO. For example, copolymerization to obtain PHD$_{75}$ using TBTPB as CTA consisted of DMAEMA (15.7 g, 99.7 mmol), HEMA (4.33 g, 33.2 mmol), TBTPB (0.12 g, 0.26 mmol), AIBN (0.01 g, 52 μmol), and 40 mL of DMSO in a 100 mL round-bottom flask equipped with a magnetic stir bar. The flask was sealed with a septum and purged with N_2 for 15 min. The flask was then placed in an oil bath preheated to 70 °C to initiate the copolymerization. The polymerization was carried out for 8 h, wherein positive N_2 pressure was maintained throughout. The polymerization was quenched by freezing the flask in liquid nitrogen, then exposing the solution to air, and diluting with THF. To remove DMSO, the solution was dialyzed against THF (10 mL of polymerization medium/300 mL of THF). The resulting solution was then precipitated into hexanes, and the filtered polymer was dried in vacuo at room temperature for 24 h. Subsequent polymerization of styrene was accomplished by using the cleaned up PHD as the macro-chain-transfer agent in DMF at 90 °C, with a styrene:PHD:AIBN molar ratio of 650:4:1. The polymerization to obtain PS/PHD$_{75}$/PS, for example, consisted of styrene (5.33 g, 51.2 mmol), PHD$_{75}$ macro-chain-transfer agent (bifunctional, M_n = 20.0 kg/mol, 0.75 g, 37.5 μmol), AIBN (0.002 g, 9.38 μmol), and 12.2 mL of DMF. The polymerization was carried out for 7 h, followed by termination, dialysis, and precipitation as described for the PHD synthesis.

Characterization. Gel permeation chromatography (GPC) was performed using a GPC system equipped with a Waters 515 HPLC solvent pump, two PLgel mixed-C columns (5 μm bead size, MW range 200−2 000 000 g/mol, Polymer Laboratories Inc.) connected in series with an Optilab DSP interferometric refractometer, and a multiangle laser light scattering (MALLS) detector (λ = 690 nm, DAWN-EOS, Wyatt Technology Corp.). The absolute molecular weight of the PS macroinitiator was obtained from GPC using THF as eluent at a flow rate of 1.0 mL/min at 40 °C given a previously reported dn/dc value.[57] GPC was performed on PHD macro-chain-transfer agents and PHD-containing block copolymers using DMF with 0.05 M LiBr[61] (Aldrich) as eluent at 60 °C; absolute molecular weights of PHD were determined using a previously reported dn/dc value of 0.1009.[45] ^{1}H NMR spectroscopy was performed in deuterated DMF on a Varian Unity+ 300 MHz NMR spectrometer. The absolute molecular weights of the block copolymers were determined from ^{1}H NMR, given the absolute molecular weight of the first block, per previous reports.[45,62] Small-angle X-ray scattering (SAXS) was performed in a long-range sample chamber,

Table 1. Physical Characteristics of PS/PHD Diblock Copolymers and PS/PHD/PS Triblock Copolymers

identifier	$M_{n,PS}$ (kg/mol)	$M_{n,PHD}$ (kg/mol)	M_w/M_n	x_{PHD}[b]	v_{PHD}[c]	x_D[d]	d_o (nm)[e]
PS/PHD_{28}	6.8[a]	5.8	1.16	0.392	0.427	0.281	18.1
$PS/PHD_{28}/PS$	4.5	15.6[a]	1.12	0.567	0.605	0.281	19.5
PS/PHD_{50}	5.4	9.8[a]	1.10	0.568	0.608	0.504	26.6
PS/PHD_{75}	6.7	14.0[a]	1.13	0.591	0.633	0.748	29.8
$PS/PHD_{75}/PS$	5.9	20.0[a]	1.19	0.540	0.584	0.751	25.7

[a] Indicates first block. PS/PHD_{28} was synthesized by ATRP while the others were made by RAFT. [b] Overall mole fraction of PHD. [c] Volume fraction of PHD; calculated using molar compositions from ^{1}H NMR and polymer densities of $\rho_{PHD75}^{54} = 1.27$ g/cm^3, $\rho_{PHD50}^{54} = 1.21$ g/cm^3, $\rho_{PHD28}^{45} = 1.20$ g/cm^3, and $\rho_{PS}^{60} = 1.05$ g/cm^3. [d] Mole fraction of DMAEMA within PHD. [e] $d = 2\pi/q^*$.

and scattered photons were collected on a 2D multiwire gas-filled detector (Molecular Metrology, Inc.). X-rays were produced by a rotating copper anode X-ray generator (Bruker Nonius; $\lambda = 1.5406$ Å) operating at 3.0 kW. Zero angle was calibrated with silver behenate ($CH_3(CH_2)_{20}COOAg$). SAXS profiles were acquired for either 1 or 2 h. SAXS experiments on the swollen block copolymer networks were performed using a liquid cell (Molecular Metrology, Inc.), with individual profiles acquired for 6 h.

All PS/PHD and PS/PHD/PS samples were fully characterized by GPC and by ^{1}H NMR. The relevant physical characteristics of the polymers used in this study are summarized in Table 1.

Swelling Studies. Phosphate buffers (0.1 M) of varying pH (pH = 4.7−8.8) were prepared using potassium phosphate monobasic (Fisher Scientific) and potassium phosphate dibasic (anhydrous, Fisher Scientific), diluted with deionized water. PS/PHD and PS/PHD/PS samples were solvent cast from THF solutions (0.2 mg/mL) to induce microphase separation, as we have previously demonstrated for PS/PHD_{28}.[45] As verified by SAXS, all block copolymers exhibit higher-order reflections consistent with the alternating lamellar morphology,[63] which one would expect given the estimated volume fractions, v_{PHD}, in Table 1. The block copolymers were weighed before they were immersed in the select phosphate buffer (100 mL) for 24 h. Subsequently, the resulting networks were reweighed and characterized by SAXS. In this manner, we were able to collect both gravimetric swelling and microdomain characteristic dimension data[29] for each network as a function of pH. To examine the swelling characteristics of the same network at subsequent pHs, the sample was first immersed in deionized water (1 L) for 6 h and then reimmersed in the next phosphate buffer (100 mL) for 24 h. The swelling behavior of each network was systematically investigated from the most basic (pH = 8.8) to the most acidic (pH = 4.7) buffer solution. Swelling behavior was not assessed in the opposite direction due to ion trapping and coordination affects associated with DMAEMA.[3]

Results and Discussion

The SAXS profiles of $PS/PHD_{28}/PS$ and those of the same $PS/PHD_{28}/PS$ sample immersed in two different phosphate buffers (pH 8.8 and pH 4.7) are shown in Figure 1a. The SAXS profile of the block copolymer in the solid state (Figure 1a-i) exhibits a narrow and intense primary peak at $q^* = 0.322$ nm^{-1} and higher-order reflections at q/q^* ratios of 2, 3, and 4, consistent with that of an alternating lamellar morphology.[63] The SAXS profile collected in the basic phosphate buffer (pH 8.8, Figure 1a-ii) exhibits a primary peak at $q^* = 0.290$ nm^{-1} and higher-order reflections at q/q^* ratios of 2 and 3. The position of the higher-order reflections indicates that its lamellar morphology is retained after swelling. The primary peak position has shifted to a lower q compared to that of the block copolymer in the solid state, which indicates that the microdomain spacing, $d = 2\pi/q^*$, is swollen relative to that in the solid state. To facilitate discussion, we define a microdomain spacing ratio, d/d_o, where d is the characteristic lamellar interdomain spacing of the swollen network and d_o is the interdomain spacing of the block copolymer in the solid state. After immersion in the pH 8.8 phosphate buffer, d/d_o for the $PS/PHD_{28}/PS$ network is 1.11. The gravimetric swelling ratio, M/M_o, was determined from the gravimetric weights of the block copolymer before, M_o, and after, M, immersion in the phosphate buffer ($M/M_o = 1.16$).

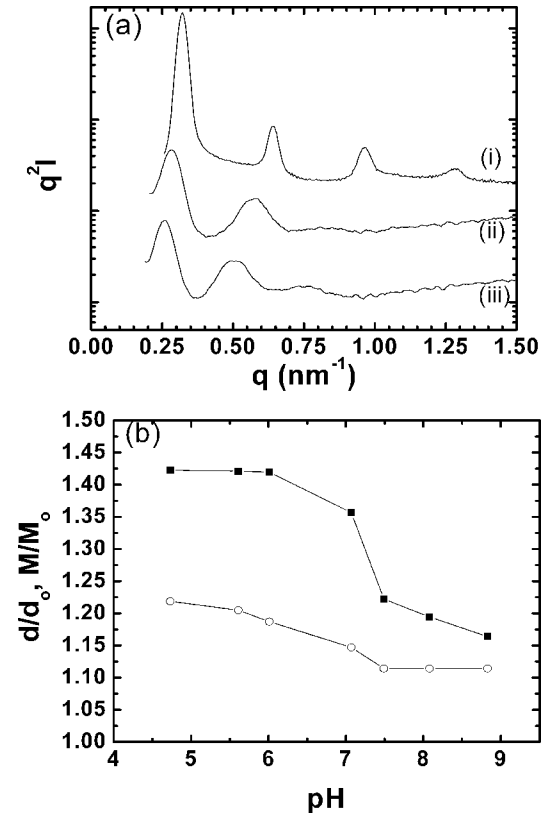

Figure 1. (a) Small-angle X-ray scattering profiles of $PS/PHD_{28}/PS$ under different conditions: (i) in the solid state, (ii) swollen in a phosphate buffer solution at pH = 8.8, and (iii) swollen in a phosphate buffer solution at pH = 4.7. (b) Gravimetric (M/M_o, ■) and microdomain (d/d_o, ○) swelling of $PS/PHD_{28}/PS$ as a function of decreasing pH.

The SAXS profile collected on $PS/PHD_{28}/PS$ that is subsequently immersed in the acidic phosphate buffer (pH 4.7, Figure 1a-iii) exhibits a primary peak at $q^* = 0.265$ nm^{-1} and higher-order reflections at q/q^* ratios of 2 and 3. As in the sample that is swollen in the basic phosphate buffer, the sample in the acidic buffer exhibits higher-order reflections consistent with that of the lamellar morphology. The primary peak position is shifted to an even lower q, which indicates further swelling of the lamellar microdomains ($d/d_o = 1.22$). Increased interdomain swelling in the acidic phosphate buffer is consistent with increases in water uptake, measured gravimetrically ($M/M_o = 1.42$). Increased swelling with decreasing solution pH is consistent with the swelling behavior that had been previously observed for cationic hydrogels.[12] We characterized the $PS/PHD_{28}/PS$ network across a range of pH values; the microdomain spacing ratio and gravimetric swelling ratio for $PS/PHD_{28}/PS$ at each pH are shown in Figure 1b. The block copolymer network behaves like a cationic hydrogel, with a large extent of swelling in acidic media and a pronounced change in swelling upon crossing the pK_a of poly(DMAEMA) at pH 7.5.[4,12,61]

It is not surprising that the SAXS profile of the swollen $PS/PHD_{28}/PS$ sample exhibits higher-order reflections consistent with that of an alternating lamellar morphology. PS is hydrophobic and glassy at ambient temperatures.[60] As a result, the PS domains do not sorb water, and they maintain their rigidity during swelling of PHD_{28}. In $PS/PHD_{28}/PS$ triblock copolymers,

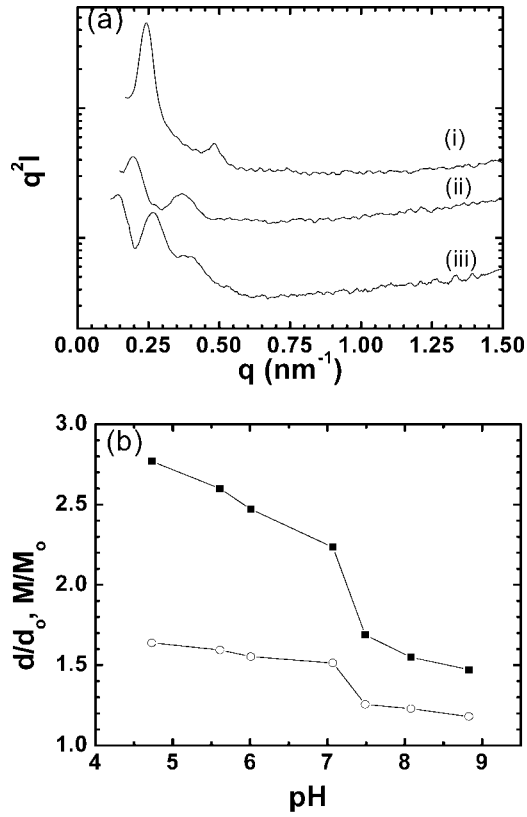

Figure 2. (a) Small-angle X-ray scattering profiles of PS/PHD$_{75}$/PS under different conditions: (i) in the solid state, (ii) swollen in a phosphate buffer solution at pH = 8.8, and (iii) swollen in a phosphate buffer solution at pH = 4.7. (b) Gravimetric (M/M_o, ■) and microdomain (d/d_o, ○) swelling of PS/PHD$_{75}$/PS as a function of decreasing pH.

the PHD segments are anchored at their ends by two neighboring glassy PS microdomains. These PS microdomains effectively serve as physical cross-links, retaining the morphology of the solid state during swelling.[28]

In order to examine the effects of the composition of PHD on the swelling behavior of PS/PHD/PS networks, we have also examined the swelling behavior of PS/PHD$_{75}$/PS. The SAXS profiles of PS/PHD$_{75}$/PS in the solid state and those of the same PS/PHD$_{75}$/PS sample immersed in buffer solutions at pH 8.8 and pH 4.7 are shown in Figure 2a. Similar to that of PS/PHD$_{28}$/PS in the solid state, the SAXS profile of PS/PHD$_{75}$/PS (Figure 2a-i) exhibits a lamellar morphology, with a primary peak at $q^* = 0.244$ nm^{-1} and a higher-order reflection at $q/q^* = 2$. Upon immersion in the basic phosphate buffer (pH 8.8; Figure 2a-ii), the sample imbibes water ($M/M_o = 1.47$), and the primary peak position in the SAXS profile of the swollen sample shifts to a lower q ($q^* = 0.207$ nm^{-1}; $d/d_o = 1.18$). The SAXS profile maintains a higher-order reflection at $q/q^* = 2$, indicating that the lamellar morphology is retained. At pH 4.7 (Figure 2a-iii), the sample takes in even more water ($M/M_o = 2.77$). The primary peak position in the SAXS profile of the swollen sample has shifted to a significantly lower q compared to that of the PS/PHD$_{75}$/PS sample in the solid state ($q^* = 0.149$ nm^{-1}; $d/d_o = 1.64$), and two higher-order reflections associated with the lamellar morphology ($q/q^* = 2$ and 3) are observed.[63] Gravimetric swelling data and microdomain spacing ratios for PS/PHD$_{75}$/PS network as a function of pH are presented in Figure 2b.

As with PS/PHD$_{28}$/PS, the PS/PHD$_{75}$/PS network displays swelling behavior that is typical of that of cationic hydrogels.[12] PS/PHD$_{75}$/PS retains both its macroscopic integrity and its microscopic lamellar morphology during swelling due to its triblock copolymer architecture in which PS domains effectively serve as glassy physical cross-links for the swellable phase. The extent of swelling observed in PS/PHD$_{75}$/PS, however, is significantly greater than that observed in PS/PHD$_{28}$/PS. We attribute this difference to the compositional difference of the swellable PHD midblock. There is significantly more DMAEMA in the midblock of PS/PHD$_{75}$/PS compared to that in PS/PHD$_{28}$/PS. At ambient temperatures, DMAEMA is more hydrophilic than HEMA.[54] As such, the incorporation of more DMAEMA into the PHD block should result in greater swelling. Further, DMAEMA can be protonated below its pK_a.[4] The additional DMAEMA present in PHD$_{75}$ results in a greater swelling change in PS/PHD$_{75}$/PS upon crossing the pK_a of poly(DMAEMA). While not surprising, we note a monotonic increase in the extent of swelling of PS/PHD/PS model networks with increasing DMAEMA content from PHD$_{28}$ to PHD$_{75}$. This result is contrary to a recent report that the swelling characteristics of PHD hydrogels plateau at 15 mol % DMAEMA.[12] The discrepancy between the two observations is likely related to differences in synthesis and, as a consequence, differences in the uniformity of comonomer and/or cross-link distributions within the networks.

To assess the importance of block copolymer architecture on the swelling behavior of PS/PHD/PS, we examined the swelling behavior of PS/PHD diblock copolymers of similar compositions. Specifically, we investigated the swelling behavior of PS/PHD$_{75}$, a lamella-forming diblock copolymer with comparable PHD composition to that of PS/PHD$_{75}$/PS. The SAXS profiles of PS/PHD$_{75}$ and of the same PS/PHD$_{75}$ sample swollen under basic (pH 8.8) and acidic (pH 4.7) conditions are shown in Figure 3a. The block copolymer exhibits a SAXS profile (Figure 3a-i) that is consistent with an alternating lamellar morphology,[63] with a primary peak at $q^* = 0.211$ nm^{-1} and a higher-order reflection at $q/q^* = 2$. When immersed in the pH 8.8 phosphate buffer, the sample swells significantly ($M/M_o = 1.60$). Correspondingly, the primary peak in the SAXS profile of the swollen PS/PHD$_{75}$ sample (Figure 3a-ii) shifts to the left ($q^* = 0.184$ nm^{-1}; $d/d_o = 1.15$), relative to that of the PS/PHD$_{75}$ diblock copolymer in the solid state. A higher order peak at $q/q^* = 2$ remains visible in the SAXS profile, suggesting that the lamellar morphology is maintained. The SAXS profile of PS/PHD$_{75}$ at pH 4.7 is shown in Figure 3a-iii. Under these conditions, we observe a significant shift in the primary peak position ($q^* = 0.120$ nm^{-1}; $d/d_o = 1.76$). Higher-order reflections are also still visible at peak ratios of $q/q^* = 2$ and 3, indicating that the network maintains its lamellar morphology even at pHs below the pK_a of poly(DMAEMA).

Microdomain spacing and gravimetric swelling data for PS/PHD$_{75}$ are presented as a function of pH in Figure 3b. Over the course of our pH experiments, PS/PHD$_{75}$ broke into many smaller pieces, most of which we were unable to recover for gravimetric analysis. This phenomenon was first observed when we immersed PS/PHD$_{75}$ in the pH 7 buffer solution, which is just below the pK_a of poly(DMAEMA).[4] PS/PHD$_{75}$ continued to break into smaller pieces with each subsequent reduction in pH. As such, the swelling data presented in Figure 3b does not include gravimetric swelling information below pH 7. We were, however, able to collect several of the smaller pieces that were still large enough for SAXS. SAXS on these smaller pieces indicate that, while the PS/PHD$_{75}$ network no longer maintains its original macroscopic integrity, the alternating lamellar morphology is retained on swelling below pH 7. As evinced by the microdomain spacing data in Figure 3b, the lamellar microdomains continue to respond to decreasing pH.

Unlike PS/PHD$_{75}$/PS, PS/PHD$_{75}$ disintegrated macroscopically because the PHD segments are not anchored by PS glassy

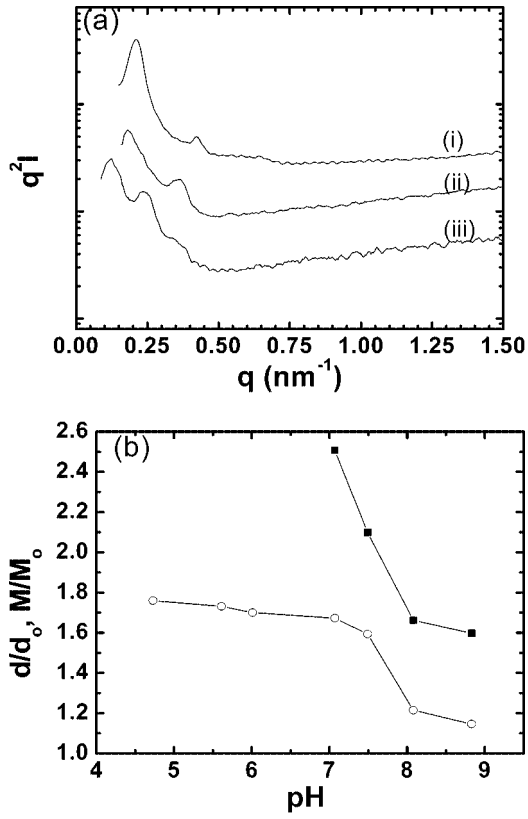

Figure 3. (a) Small-angle X-ray scattering profiles of PS/PHD$_{75}$ under different conditions: (i) in the solid state, (ii) swollen in a phosphate buffer solution at pH = 8.8, and (iii) swollen in a phosphate buffer solution at pH = 4.7. (b) Gravimetric (M/M_o, ■) and microdomain (d/d_o, ○) swelling of PS/PHD75 as a function of decreasing pH. Below pH 7, PS/PHD$_{75}$ loses macroscopic integrity and is no longer suitable for macroscopic assessment. PS/PHD$_{75}$ maintains a lamellar microstructure throughout the experiment.

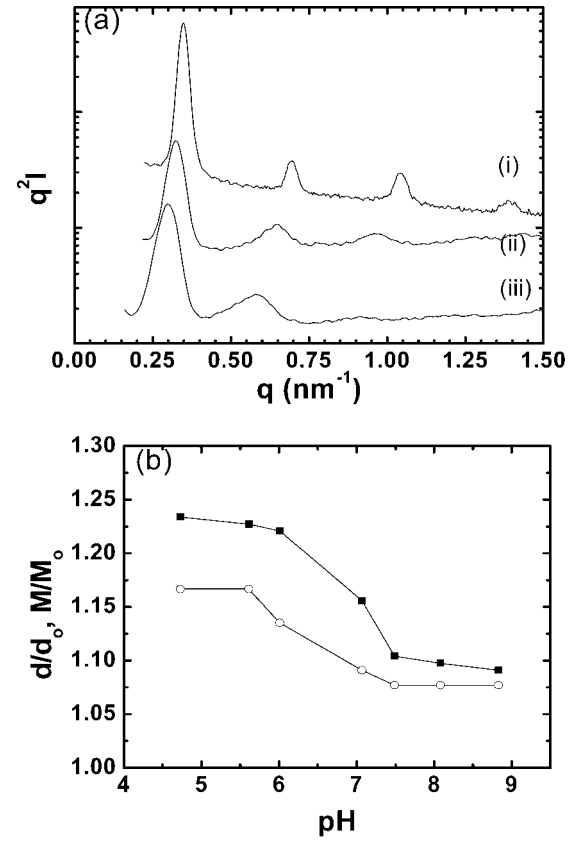

Figure 4. (a) Small-angle X-ray scattering profiles of PS/PHD$_{28}$ under different conditions: (i) in the solid state, (ii) swollen in a phosphate buffer solution at pH = 8.8, and (iii) swollen in a phosphate buffer solution at pH = 4.7. (b) Gravimetric (M/M_o, ■) and microdomain (d/d_o, ○) swelling of PS/PHD$_{28}$ as a function of decreasing pH.

microdomains on both ends. Microscopically, the periodic lamellar structure is retained, presumably because the osmotic pressure due to water uptake and the electrostatic repulsion generated by protonated DMAEMA units within facing lamellae is not significant enough to force complete separation of the diblock copolymer lamellae.[65] As such, the loss of macroscopic integrity in PS/PHD$_{75}$ is likely to originate at structural defects, such as grain boundaries that were predefined during solvent casting of the solid-state sample.[66]

We have also examined the swelling behavior of PS/PHD$_{50}$. Briefly, the PS/PHD$_{50}$ sample imbibes water (M/M_o = 1.22, d/d_o = 1.16) when swollen in the pH 8.8 phosphate buffer. Similar to PS/PHD$_{75}$, PS/PHD$_{50}$ loses macroscopic integrity upon crossing the pK_a of p(DMAEMA). SAXS analysis performed on collected pieces of the PS/PHD$_{50}$ sample confirm that its alternating lamellar morphology is retained even after the loss of macroscopic integrity. Further, the PS/PHD$_{50}$ sample continues to undergo microdomain swelling characteristic of a cationic hydrogel (d/d_o = 1.36 at pH 4.7). We note that the swelling in PS/PHD$_{50}$ is less than that of PS/PHD$_{75}$ due to the fact that less DMAEMA is present in the PS/PHD$_{50}$ sample. In both cases, the swelling that occurs upon protonation of DMAEMA are significant enough to macroscopically destabilize the samples.

Finally, we examined the swelling behavior of PS/PHD$_{28}$. The SAXS profiles of PS/PHD$_{28}$ and those of the same sample immersed in buffers of different pH (pH 8.8 and pH 4.7) are shown in Figure 4a. Similar to its triblock copolymer counterpart, the SAXS profile of PS/PHD$_{28}$ in the solid state (Figure 4a-i) indicates that the sample adopts a lamellar morphology, with a primary peak position of q^* = 0.348 nm^{-1} and higher-order reflections at q/q^* ratios of 2, 3, and 4. Upon immersion in the basic phosphate buffer (pH 8.8, Figure 4a-ii), the primary peak position shifts to a lower q (q^* = 0.323 nm^{-1}; d/d_o = 1.08), but the SAXS profile maintains higher-order reflections at q/q^* ratios of 2 and 3, consistent with that of a lamellar morphology.[63] Upon immersion in the acidic phosphate buffer (pH 4.7, Figure 4a-iii), the primary peak position shifts to even smaller q (q^* = 0.298 nm^{-1}; d/d_o = 1.17). The microdomain spacing ratio of PS/PHD$_{28}$ is shown, as a function of buffer pH, in Figure 4b. Gravimetric data, which was also collected over the full pH range, are also shown in Figure 4b. In contrast to PS/PHD$_{75}$ and PS/PHD$_{50}$, PS/PHD$_{28}$ does not lose its macroscopic integrity during the entire swelling process.

It has been widely assumed that a triblock copolymers with two hydrophobic end blocks are necessary to provide structural integrity to model networks.[21–28] Diblock copolymers, on the other hand, are incapable of anchoring the swellable block so macroscopic disintegration is generally expected. The swelling experiments of PS/PHD$_{75}$ and PS/PHD$_{50}$ confirm that diblock copolymer networks are indeed destabilized upon protonation of the ionic component. In the case of PS/PHD$_{28}$, however, the diblock copolymer architecture is sufficient to preserve the macroscopic integrity of the network when swollen across 4 decades of pH. When protonated, PHD$_{75}$ has a higher charge density than PHD$_{28}$. The water driven into the PHD phase thus generates a higher osmotic pressure in PHD$_{75}$ compared to PHD$_{28}$. From the swelling behavior of PS/PHD$_{28}$, PS/PHD$_{50}$, and PS/PHD$_{75}$, it appears that there exists a threshold concentration of DMAEMA within the swellable block that governs whether the diblock copolymer architecture can suitably withstand the osmotic pressure generated within the network upon

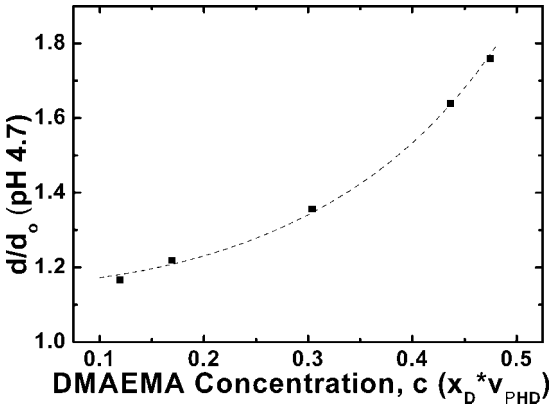

Figure 5. Normalized microdomain expansion in networks of PS/PHD and PS/PHD/PS at pH 4.7, expressed in terms of the DMEAMA unit density. The dashed curve represents a fit to the data derived from the functional form of a modified Brannon-Peppas model for ionic hydrogels (eq 3).[64]

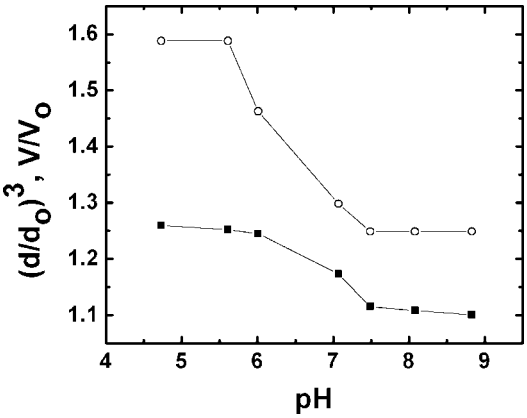

Figure 6. Volume expansion of PS/PHD_{28} as a function of decreasing pH, as determined by SAXS data assuming isotropic swelling, $(d/d_o)^3$ (○), and as predicted by gravimetric data, V/V_o (■).

DMAEMA protonation. Given that the DMAEMA content within PHD_{28} is relatively low, PS/PHD_{28} is able to maintain its macroscopic integrity during swelling. Its swelling behavior thus mirrors that of the physically cross-linked $PS/PHD_{28}/PS$ triblock copolymer network.

The swelling properties of PS/PHD and PS/PHD/PS networks are related to four factors: the relative volume fraction of the PHD block (v_{PHD}), the fraction of DMAEMA in the PHD block (x_D), the overall molecular weight of the PHD block, and the block copolymer architecture. By normalizing microdomain swelling against the characteristic domain size of the block copolymer in the solid state (d/d_o), we have accounted for differences in the molecular weight of the block copolymers. The overall composition of DMAEMA in the network can be described by the volume fraction of the PHD block and the composition DMAEMA within the PHD block ($c = v_{PHD}x_D$). In Figure 5, we have plotted the microdomain spacing ratio (d/d_o) at pH 4.7 as a function of the overall DMAEMA composition. The microdomain swelling properties in PS/PHD and PS/PHD/PS networks are strongly correlated with the DMAEMA concentration. As observed in Figure 5, a 35% increase in the overall DMAEMA concentration in the network results in a 4.5-fold increase in the swelling response at pH 4.7. Above the pK_a of poly(DMAEMA)—more specifically, at pH 8.8—DMAEMA is not protonated[9] and therefore only contributes toward the hydrophilicity of the network.[54] The dependence of swelling on the overall DMAEMA composition is therefore less apparent at basic conditions.

We have chosen to assess the dependence of microdomain swelling on the overall DMAEMA composition in our block copolymer networks with models derived for traditional, chemically cross-linked hydrogels. Most useful in this regard is a swelling model, proposed by Brannon-Peppas et al., that describes the swelling equilibrium of ionic hydrogels as a balance between the ionic chemical potential and the combined mixing and elastic potentials of the hydrogel.[64] The Brannon-Peppas model assumes that all cross-links are point cross-links connected to four extended polymer arms and that all cross-links are introduced in the swollen state.[64] Since our cross-links are introduced in the dry state, we use the more appropriate Flory−Rehner model to describe mixing and elastic potentials,[67] while retaining the Brannon-Peppas derivation of ionic potential.[64] The complete swelling equilibrium condition of our networks, expressed in terms of the concentration of the ionizable component, c, can thus be written as eq 1:

$$\left(\frac{K_b}{10^{pH-14}+K_b}\right)^2\left(\frac{V_1}{4I}\right)c^2 = \ln(1-v_2)+v_2+\chi(v_2)^2+\left(\frac{V_1}{vM_c}\right)\left(1-\frac{2M_c}{M_n}\right)\left(v_2^{1/3}-\frac{v_2}{2}\right) \quad (1)$$

where V_1 is the molar volume of the swelling agent, I is the ionic strength of the solution, v_2 is the polymer volume fraction in the network at equilibrium, v is the specific volume of the polymer, χ is the Flory interaction parameter between polymer and solvent, M_c is the molecular weight between cross-links, and M_n is the number-average molecular weight before cross-linking. For the purpose of evaluating our PS/PHD and PS/PHD/PS networks, we assume that M_c is accounted for by normalizing the microdomain swelling of each lamellar-forming network against the characteristic microdomain spacing in the solid state. In a particular buffer of known pH, eq 1 simplifies into an equation of two variables, c and v_2. While swelling within individual lamella is undoubtedly one-dimensional, macroscopic swelling of PS/PHD and PS/PHD/PS networks occur three dimensionally because the grains of lamellae have no preferential orientation. Given that macroscopic swelling is isotropic, the one-dimensional microdomain spacing ratio can be related to the equilibrium polymer volume fraction as shown in eq 2:

$$\left(\frac{d}{d_o}\right)^3 \approx \frac{1}{v_2} \quad (2)$$

As a further approximation, we simplify our model in the limit of large swelling (small v_2),[67] as shown in eq 3, where a and b are unitless constants.

$$\left(\frac{d}{d_o}\right)^{-1} \approx a - bc^2 \quad (3)$$

Subjecting our data collected at pH 4.7 to a best fit of eq 3 yields $a = 0.866$ and $b = 1.33$ (correlation coefficient = 0.996). In Figure 5, the dashed curve represents the fit according to eq 3 to the microdomain spacing ratio data. The simplified model adequately describes our data for amphiphilic PS/PHD and PS/PHD/PS networks. Further, that the microdomain swelling behavior of diblock and triblock copolymers can be modeled together with good agreement suggests that architectural differences do not significantly affect the microdomain swelling behavior of the lamellar structures within our networks.

Finally, Figure 6 compares the volume expansion of PS/PHD_{28} as determined by SAXS (○; $(d/d_o)^3$ assuming isotropic expansion) with that derived from gravimetric measurements (■; V/V_o). The volume expansion from gravimetric data was calculated assuming that the volume occupied by the PS block and that by the swollen phase are additive given the density of

water and that of the neat block copolymer, which was calculated as the weighted average of the densities of each block.[45,54,60] Across the entire pH range, the volume expansion as determined by SAXS is greater than that predicted from the gravimetric data. This observation is true for all the diblock and triblock copolymer networks examined in this study. In accordance with the lattice models of polymer−solvent mixing,[66] the discrepancy between the gravimetric and SAXS swelling data suggests an increase in free volume within the samples when swollen. Similar free volume effects have been observed during the limited swelling of DMAEMA-containing hydrogels with hydrophobic groups.[69] Further, we observe that the free volume in swollen PS/PHD or PS/PHD/PS samples decreases with increasing DMAEMA content within PHD and is generally not affected by pH. More specifically, the volume expansion of PS/PHD_{28} and PS/PHD_{28}/PS as measured by SAXS is 1.9 times greater (standard deviation = ±0.2) than that predicted by the gravimetric data. In contrast, the volumetric expansion of PS/PHD_{50} is 1.7 times greater (standard deviation = ±0.3) than the gravimetric volume expansion, and the volumetric expansion of PS/PHD_{75} and PS/PHD_{75}/PS is 1.4 times greater (standard deviation = ±0.3) than the gravimetric volume expansion. Given that the free volume present in PS/PHD or PS/PHD/PS networks is not significantly affected by pH and therefore not directly related to the amount of water present in the sample, we are left to speculate that the change in free volume is largely related to the Flory interaction parameter, χ, between the polymer and water. For DMAEMA-containing polymers in water, it has been demonstrated that χ is highly dependent on the DMAEMA content of the polymer.[70] The incorporation of HEMA into PHD domains results in an increase in χ between PHD and water, thus increasing free volume within the swellable component of the network.

Conclusions

We have successfully synthesized a series of PS/PHD diblock copolymers and PS/PHD/PS triblock copolymers with varying DMAEMA content by either RAFT or ATRP. These block copolymers microphase separate to form well-ordered lamellar structures in the solid state, with glassy PS domains serving to limit swelling of PHD upon immersion in buffers of varying pH. PS/PHD/PS and PS/PHD networks are shown to be pH-responsive, and the magnitude of their pH responsive can be controlled synthetically by adjusting the DMAEMA content. When PS/PHD/PS triblock copolymers are swollen in water, PS domains serve as physical cross-links that hold the network together. In contrast, PS domains within PS/PHD diblock copolymers are not capable of serving as physical cross-links. As such, PS/PHD diblock copolymers with high DMAEMA content (PS/PHD_{75} or PS/PHD_{50}) fall apart after protonation of DMAEMA units. While we observe a loss of macroscopic integrity for these diblock copolymers, the lamellar microdomains within the samples continue to exhibit pH response characteristic of cationic hydrogels. Moreover, we have demonstrated that the diblock copolymer network comprised PHD_{28} are capable of withstanding the osmotic pressure induced by protonation of the DMAEMA units. As a result, this diblock copolymer network exhibits microdomain and gravimetric swelling behavior equivalent to what has been observed for physically cross-linked triblock copolymer networks.

Acknowledgment. This work is funded by the National Science Foundation (NSF CAREER DMR-0753148). Support from the Keck Foundation and Texas Materials Institute is also gratefully acknowledged. K.B.G. acknowledges the NSF for a graduate fellowship. S.R.M. acknowledges the NSF for an REU supplement. B.S.S. acknowledges the Petroleum Research Fund of the American Chemical Society. We thank Dr. Chris Bielawski for access to GPC.

References and Notes

(1) Dong, L.; Agarwal, A. K.; Beebe, D. J.; Jiang, H. *Nature (London)* **2006**, *442*, 551–554.
(2) Du, R.; Zhao, J. *J. Appl. Polym. Sci.* **2004**, *91*, 2721–2728.
(3) Yilmaz, Z.; Akkas, P. K.; Sen, M.; Guven, O. *J. Appl. Polym. Sci.* **2006**, *102*, 6023–6027.
(4) Van de Wetering, P.; Moret, E. E.; Schuurmans-Nieuwenbroek, N. M. E.; Van Steenbergen, M. J.; Hennink, W. E. *Bioconjugate Chem.* **1999**, *10*, 589–597.
(5) Brahim, S.; Narinesingh, D.; Guiseppi-Elie, A. *Biomacromolecules* **2003**, *4*, 1224–1231.
(6) Satish, C. S.; Shivakumar, H. G. *J. Macromol. Sci., Part A: Pure Appl. Chem.* **2007**, *44*, 379–387.
(7) Traitel, T.; Cohen, Y.; Kost, J. *Biomaterials* **2000**, *21*, 1679–1687.
(8) Fournier, D.; Hoogenboom, R.; Thijs, H. M. L.; Paulus, R. M.; Schubert, U. S. *Macromolecules* **2007**, *40*, 915–920.
(9) Kroupova, J.; Horak, D.; Pachernik, J.; Dvorak, P.; Slouf, M. *J. Bio. Mater. Res., Part B: Appl. Biomater.* **2006**, *76B*, 315–325.
(10) Siegel, R. A.; Firestone, B. A. *Macromolecules* **1988**, *21*, 3254–9.
(11) Traitel, T.; Kost, J.; Lapidot, S. A. *Biotechnol. Bioeng.* **2003**, *84*, 20–28.
(12) Brahim, S.; Narinesingh, D.; Guiseppi-Elie, A. *Biomacromolecules* **2003**, *4*, 497–503.
(13) Herber, S.; Eijkel, J.; Olthuis, W.; Bergveld, P.; van den Berg, A. *J. Chem. Phys.* **2004**, *121*, 2746–2751.
(14) Kwok, A. Y.; Qiao, G. G.; Solomon, D. H. *Polymer* **2004**, *45*, 4017–4027.
(15) Kopecek, J.; Yang, J. *Polym. Int.* **2007**, *56*, 1078–1098.
(16) Haraguchi, K.; Takehisa, T. *Adv. Mater.* **2002**, *14*, 1120–1124.
(17) Huglin, M. B.; Zakaria, M. B. *Polymer* **1984**, *25*, 797–802.
(18) Liu, R.; Oppermann, W. *Macromolecules* **2006**, *39*, 4159–4167.
(19) Martin-Gomis, L.; Cuervo-Rodriguez, R.; Fernandez-Monreal, M. C.; Madruga, E. L.; Fernandez-Garcia, M. *J. Polym. Sci., Part A: Polym. Chem.* **2003**, *41*, 2659–2666.
(20) Kishi, H.; Naitou, T.; Matsuda, S.; Murakami, A.; Muraji, Y.; Nakagawa, Y. *J. Polym. Sci., Part B: Polym. Phys.* **2007**, *45*, 1425–1434.
(21) Triftaridou, A. I.; Hadjiyannakou, S. C.; Vamvakaki, M.; Patrickios, C. S. *Macromolecules* **2002**, *35*, 2506–2513.
(22) Krasia, T. C.; Patrickios, C. S. *Macromolecules* **2006**, *39*, 2467–2473.
(23) Achilleos, M.; Krasia-Christoforou, T.; Patrickios, C. S. *Macromolecules* **2007**, *40*, 5575–5581.
(24) Themistou, E.; Patrickios, C. S. *Macromolecules* **2007**, *40*, 5231–5234.
(25) Triftaridou, A. I.; Kafouris, D.; Vamvakaki, M.; Georgiou, T. K.; Krasia, T. C.; Themistou, E.; Hadjiantoniou, N.; Patrickios, C. S. *Polym. Bull.* **2007**, *58*, 185–190.
(26) Triftaridou, A. I.; Vamvakaki, M.; Patrickios, C. S. *Biomacromolecules* **2007**, *8*, 1615–1623.
(27) Vamvakaki, M.; Patrickios, C. S.; Lindner, P.; Gradzielski, M. *Langmuir* **2007**, *23*, 10433–10437.
(28) Nykaenen, A.; Nuopponen, M.; Laukkanen, A.; Hirvonen, S.-P.; Rytelae, M.; Turunen, O.; Tenhu, H.; Mezzenga, R.; Ikkala, O.; Ruokolainen, J. *Macromolecules* **2007**, *40*, 5827–5834.
(29) Topham, P. D.; Howse, J. R.; Crook, C. J.; Gleeson, A. J.; Bras, W.; Armes, S. P.; Jones, R. A. L.; Ryan, A. J. *Macromol. Symp.* **2007**, *256*, 95–104.
(30) Xu, C.; Fu, X.; Fryd, M.; Xu, S.; Wayland, B. B.; Winey, K. I.; Composto, R. J. *Nano Lett.* **2006**, *6*, 282–287.
(31) La, Y.-H.; Edwards, E. W.; Park, S.-M.; Nealey, P. F. *Nano Lett.* **2005**, *5*, 1379–1384.
(32) Ludwigs, S.; Schmidt, K.; Krausch, G. *Macromolecules* **2005**, *38*, 2376–2382.
(33) Xu, C.; Wayland, B. B.; Fryd, M.; Winey, K. I.; Composto, R. J. *Macromolecules* **2006**, *39*, 6063–6070.
(34) Leibler, L. *Macromolecules* **1980**, *13*, 1602–17.
(35) Matyjaszewski, K.; Xia, J. *Chem. Rev.* **2001**, *101*, 2921–2990.
(36) Kamigaito, M.; Ando, T.; Sawamoto, M. *Chem. Rev.* **2001**, *101*, 3689–3745.
(37) Chiefari, J.; Chong, Y. K.; Ercole, F.; Krstina, J.; Jeffery, J.; Le, T. P. T.; Mayadunne, R. T. A.; Meijs, G. F.; Moad, C. L.; Moad, G.; Rizzardo, E.; Thang, S. H. *Macromolecules* **1998**, *31*, 5559–5562.
(38) Moad, G.; Rizzardo, E.; Thang, S. H. *Aust. J. Chem.* **2005**, *58*, 379–410.
(39) Sumerlin, B. S.; Lowe, A. B.; Thomas, D. B.; Convertine, A. J.; Donovan, M. S.; McCormick, C. L. *J. Polym. Sci., Part A: Polym. Chem.* **2004**, *42*, 1724–1734.
(40) Sumerlin, B. S.; Lowe, A. B.; Thomas, D. B.; McCormick, C. L. *Macromolecules* **2003**, *36*, 5982–5987.

(41) Convertine, A. J.; Sumerlin, B. S.; Thomas, D. B.; Lowe, A. B.; McCormick, C. L.*Macromolecules* **2003**, *36*, 4679–4681.
(42) Thomas, D. B.; Sumerlin, B. S.; Lowe, A. B.; McCormick, C. L. *Macromolecules* **2003**, *36*, 1436–1439.
(43) Donovan, M. S.; Lowe, A. B.; Sumerlin, B. S.; McCormick, C. L. *Macromolecules* **2002**, *35*, 4123–4132.
(44) Sumerlin, B. S.; Donovan, M. S.; Mitsukami, Y.; Lowe, A. B.; McCormick, C. L. *Macromolecules* **2001**, *34*, 6561–6564.
(45) Guice, K. B.; Loo, Y.-L. *Macromolecules* **2006**, *39*, 2474–2480.
(46) Teoh, R. L.; Guice, K. B.; Loo, Y.-L. *Macromolecules* **2006**, *39*, 8609–8615.
(47) Monge, S.; Darcos, V.; Haddleton, D. M. *J. Polym. Sci., Part A: Polym. Chem.* **2004**, *42*, 6299–6308.
(48) Jin, X.; Shen, Y.; Zhu, S. *Macromol. Mater. Eng.* **2003**, *288*, 925–935.
(49) Lee, S. B.; Russell, A. J.; Matyjaszewski, K. *Biomacromolecules* **2003**, *4*, 1386–1393.
(50) Mao, B.; Gan, L.-H.; Gan, Y.-Y.; Li, X.; Ravi, P.; Tam, K.-C. *J. Polym. Sci., Part A: Polym. Chem.* **2004**, *42*, 5161–5169.
(51) Zhang, X.; Xia, J.; Matyjaszewski, K. *Macromolecules* **1998**, *31*, 5167–5169.
(52) Sahnoun, M.; Charreyre, M.-T.; Veron, L.; Delair, T.; D'Agosto, F. *J. Polym. Sci., Part A: Polym. Chem.* **2005**, *43*, 3551–3565.
(53) Xiong, Q.; Ni, P.; Zhang, F.; Yu, Z. *Polym. Bull.* **2004**, *53*, 1–8.
(54) Guice, K. B.; Loo, Y.-L. *Macromolecules* **2007**, *40*, 9053–9058.
(55) Weaver, J. V. M.; Bannister, I.; Robinson, K. L.; Bories-Azeau, X.; Armes, S. P.; Smallridge, M.; McKenna, P. *Macromolecules* **2004**, *37*, 2395–2403.
(56) Oae, S. Y. T.; Okabe, T. *Tetrahedron* **1972**, *28*, 3203–3216.
(57) Becke, F. H. H. *Badische Anilin & Soda-Fabrik Aktiengesellschaft*; Germany, 1968.
(58) Asgarzadeh, F. B., E.; Chaumont, P. *Polym. Prepr. (Am. Chem. Soc., Div. Polym. Chem.)* **1999**, *40*, 899–900.
(59) Tsarevsky, N. V.; Pintauer, T.; Matyjaszewski, K. *Macromolecules* **2004**, *37*, 9768–9778.
(60) *Polymer Handbook*, 4th ed.; Brandrup, J., Immergut, E. H., Grulke, E. A., Eds.; Wiley-Interscience: New York, 1999.
(61) Coppola, G.; Fabbri, P.; Pallesi, B.; Bianchi, U. *J. Appl. Polym. Sci.* **1972**, *16*, 2829–2834.
(62) Bucholz, T. L.; Loo, Y.-L. *Macromolecules* **2006**, *39*, 6075–6080.
(63) Shibayama, M.; Hashimoto, T.; Kawai, H. *Macromolecules* **1983**, *16*, 16–28.
(64) Brannon-Peppas, L.; Peppas, N. A. *Polym. Bull.* **1988**, *20*, 285–9.
(65) Bendejacq, D.; Ponsinet, V.; Joanicot, M. *Eur. Phys. J. E* **2004**, *13*, 3–13.
(66) Cohen, Y.; Thomas, E. L. *Macromolecules* **2003**, *36*, 5265–5270.
(67) Flory, P. J.; Rehner, J., Jr *J. Chem. Phys.* **1943**, *11*, 521–6.
(68) Sanchez, I. C.; Lacombe, R. H. *Macromolecules* **1978**, *11*, 1145–56.
(69) Suevegh, K.; Domjan, A.; Vanko, G.; Ivan, B.; Vertes, A. *Macromolecules* **1998**, *31*, 7770–7775.
(70) Emileh, A.; Vasheghani-Farahani, E.; Imani, M. *Eur. Polym. J.* **2007**, *43*, 1986–1995.

MA8003746